Acta Crystallographica Section D
Biological Crystallography
ISSN 0907-4449

Structure of spinach acetohydroxyacid isomeroreductase complexed with its reaction product dihydroxymethylvalerate, manganese and (phospho)-ADP-ribose

Karine Thomazeau,[a] Renaud Dumas,[b] Frédéric Halgand,[a]† Eric Forest,[a] Roland Douce[b] and Valérie Biou[a]*

[a]Institut de Biologie Structurale Jean-Pierre Ebel (UMR 5045), CNRS/CEA/Université Joseph Fourier, 41 Rue Jules Horowitz, F-38027 Grenoble CEDEX, France, and [b]Unité Mixte CNRS/Aventis (UMR 1932), Aventis CropScience, 14–20 Rue Pierre Baizet, F-69263 Lyon CEDEX 09, France

† Present address: CNRS, Institut de Chemie des Substances Naturelles, 1 avenue de la Terrasse, F-9 1198 Gif sur Yvette, France.

Correspondence e-mail: valerie.biou@ibs.fr

Received 24 September 1999
Accepted 31 January 2000

PDB Reference: Isomeroreductase–dihydroxymethylvalerate complex, 1qmg.

Acetohydroxyacid isomeroreductase catalyses a two-step reaction composed of an alkyl migration followed by an NADPH-dependent reduction. Both steps require a divalent cation and the first step has a strong preference for magnesium. Manganese ions are highly unfavourable to the reaction: only 3% residual activity is observed in the presence of this cation. Acetohydroxyacid isomeroreductase has been crystallized with its substrate, 2-aceto-2-hydroxybutyrate (AHB), Mn^{2+} and NADPH. The 1.6 Å resolution electron-density map showed the reaction product (2,3-dihydroxy-3-methylvalerate, DHMV) and a density corresponding to (phospho)-ADP-ribose instead of the whole $NADP^+$. This is one of the few structures of an enzyme complexed with its reaction product. The structure of this complex was refined to an R factor of 19.3% and an R_{free} of 22.5%. The overall structure of the enzyme is very similar to that of the complex with the reaction-intermediate analogue IpOHA [*N*-hydroxy-*N*-isopropyloxamate; Biou *et al.* (1997), *EMBO J.* **16**, 3405–3415]. However, the active site shows some differences: the nicotinamide is cleaved and the surrounding amino acids have rearranged accordingly. Comparison between the structures corresponding to the reaction intermediate and to the end of the reaction allowed the proposal of a reaction scheme. Taking this result into account, the enzyme was crystallized with Ni^{2+} and Zn^{2+}, for which only 0.02% residual activity were measured; however, the crystals of AHB/Zn/NADPH and of AHB/Ni/NADPH also contain the reaction product. Moreover, mass-spectrometry measurements confirmed the cleavage of nicotinamide.

1. Abbreviations

AHB, 2-aceto-2-hydroxybutyrate; NADPH, nicotinamide adenine dinucleotide; Ir, acetohydroxyacid isomeroreductase; IpOHA, *N*-hydroxy-*N*-isopropyloxamate; DHMV, 2,3-dihydroxy-3-methylvalerate; MALDI, matrix-assisted laser desorption ionisation; EDTA, ethylene-diamine tetra-acetic acid; r.m.s.d., root-mean-square deviation.

2. Introduction

There is a time difference between biochemistry and protein crystallography. It is not only a time difference but also a time stretch: enzymatic reactions are measured on minute scales, while a protein crystal takes on average several days to grow to a diffracting size. Therefore, a condition that seems inactive on a biochemical time scale may well allow the completion of the reaction in the time-lapse of 5 d. This is what we have observed during our quest for the initial reaction stage of

Table 1
Data-collection and processing details.

Cation	Mn^{2+}	Ni^{2+}	Zn^{2+}
Wavelength (Å)	0.984	0.83	0.83
Unit-cell parameters (Å, °)	110.8, 61.2, 161.7, 90, 95.0, 90	112.5, 112.5, 338.6, 90, 90, 120	183.7, 65.6, 90.6, 90, 90, 90
Space group	$P2_1$	$P3_121$	$P2_12_12$
Resolution (Å)	26–1.60	2.5 (detector edge)	2.04 (detector edge)
R_{sym}† (at resolution edge)	0.054 (0.096)	0.086 (0.220)	0.047 (0.098)
No. of unique reflections	299230	86613	68553
Completeness (edge) (%)	96.6 (96.6)	99.6 (99.7)	96.6 (95.9)
Multiplicity (edge)	2.9 (2.9)	4.6 (4.7)	3.7 (3.4)
Asymmetric unit content	4 monomers	4 monomers	2 monomers
Solvent content (%)	54	48	41
MR R factor‡	0.377 (10–3 Å)	0.326 (30–4 Å)	0.46 (30–2 Å)§
Refinement state	R = 0.193; R_{free} = 0.225	Not refined	Not refined

† $R_{sym} = \sum |I - \langle I \rangle| / \sum |I|$, where I is the intensity of a given reflection and $\langle I \rangle$ is the average intensity of symmetry-related reflections. ‡ The R factor for the molecular-replacement solution. $R = \sum ||F_o| - k|F_c|| / \sum |F_o|$, where $|F_o|$ and $|F_c|$ are the observed and calculated structure-factor amplitudes, respectively, for a given reflection (see §3 for molecular-replacement procedure). § The Zn^{2+} data had a unit cell quite similar to that of a preceding data set, so molecular replacement was skipped and this R-factor value corresponds to the starting value from molecular replacement in *X-PLOR*.

acetohydroxyacid isomeroreductase. Our aim was to crystallize the enzyme complexed with its substrate in an inactive state, to trigger the reaction in a second step and to observe the different reaction steps. However, the time required to obtain crystals allowed the reaction to proceed, even at a slow rate. As a result, we observed the reaction product in the active site of the enzyme. This is one of only ten different proteins complexed with their reaction products according to a search of the Protein Data Bank.

2.1. Catalysed reaction and specificity

Acetohydroxyacid isomeroreductase (E.C. 1.1.1.86) is the second enzyme of a catalytic chain leading to the synthesis of the branched side-chain amino acids valine, leucine and isoleucine. All the enzymes in this catalytic chain have specificity for two substrates differing by a methyl group. The isomeroreductase catalyses a two-step reaction (Fig. 1): firstly, an alkyl function is transferred from the central C2 to distal C3; secondly, the O atom on C2 is reduced to a hydroxyl by an NADPH-dependent reaction. Both steps require the presence of a divalent cation. The reaction catalysed is highly specific in several ways: it is stereospecific (Sylvester & Stevens, 1979), it has a strong preference for NADPH *versus* NADH (Dumas *et al.*, 1992) and it has a strong preference for magnesium *versus* other divalent cations. Dumas *et al.* (1995) showed the binding of two divalent cations in the enzyme. The role of the cations was shown to be both structural and catalytic: substrate binding cannot occur without the addition of two cations (Halgand *et al.*, 1999) and no reaction is observed in the complete absence of cation (this work). Both cations bind to two highly conserved regions of the isomeroreductase sequences, termed regions III and IV (Dumas *et al.*, 1995). The crystallographic structure showed that cation 1 binds only to region III (Asp315 and Glu319), while cation 2 binds to both regions III (Asp315) and IV (Glu492 and Glu496; Biou *et al.*, 1997). Both parts of the reaction have different cation specificities: the isomerization reaction is highly magnesium-dependent, while the reduction reaction takes place equally well with manganese or cobalt. Mutations in region III impair both reactions, while mutation of Glu492 to Asp leaves the reduction reaction almost unaffected (Dumas *et al.*, 1995).

Specific inhibitors have been known to have a herbicidal property, preventing the plant from synthesizing amino acids. One of them is *N*-hydroxy-*N*-isopropyloxamate (IpOHA), which is a competitive inhibitor and an analogue to the reaction intermediate (Fig. 1).

2.2. Enzyme structure

The spinach isomeroreductase is a dimer of 116 kDa. There is a strong homology among plant enzymes, but only a few residues are conserved between plants and microorganisms (Dumas *et al.*, 1995). Those residues were shown to be essential for the enzyme structure or function. The structure of the complex between the spinach enzyme, magnesium ions, NADPH and intermediate analogue IpOHA has been solved to 1.65 Å (Biou *et al.*, 1997). The isomeroreductase monomer is composed of two sequential domains. The amino-terminal α/β domain, comprising a Rossmann fold, binds the NADPH cofactor. The carboxy-terminal all-α domain makes up the dimer interface, mainly through a 140 amino-acid region which is specific to plants. The active site is nested at the interface of the two domains, with a majority of residues belonging to the C-terminal domain. This structure revealed a situation close to the reaction intermediate.

2.3. Purpose of the study

Here, we present the 1.6 Å resolution structure of the isomeroreductase complexed to its reaction product, manganese ions and a degradation product of $NADP^+$, (phospho)-ADP-ribose. The enzyme was crystallized in the presence of its substrate and NADPH. In order to understand the kinetics of the appearance of the product in the crystal, we carried out reaction measurements which revealed that, although slow, the reaction did occur even with 'unfavourable' cations. In addition, mass-spectrometry measurements were performed to help to identify the compound in the active site.

3. Methods

3.1. Enzyme production, purification and crystallization

The enzyme was overexpressed in *Escherichia coli* and purified as previously described (Dumas *et al.*, 1992).

Three crystallization conditions were set up with different divalent cations in order to try to obtain complexes of the enzyme with its substrate 2-aceto-2-hydroxybutyrate (AHB). The enzyme was crystallized from 1.8 *M* ammonium sulfate in 0.1 *M* Tris–HCl at pH 7.2 (Dumas *et al.*, 1994) in the presence of AHB, NADPH (ten of each ligand molecules per enzyme monomer) and Mn^{2+} (100 ions per enzyme monomer). The

Zn^{2+} and Ni^{2+} complexes were crystallized under similar conditions using the same cation-to-enzyme ratio. Table 1 gives the unit cell and space group for each of the complexes.

3.2. Activity measurements

Acetohydroxyacid isomeroreductase activity with different divalent cations (Mg^{2+}, Mn^{2+}, Ni^{2+}, Zn^{2+}) was determined in 50 m*M* Tris–HCl buffer pH 8 with 400 µ*M* NADPH and either 5 m*M* $MgCl_2$, $MnCl_2$, $NiCl_2$ or 0.5 m*M* $ZnCl_2$, in a final volume of 1 ml. The protein concentration was 35 µg ml^{-1} (0.6 µ*M*). In addition, one measurement was carried out without adding any cation to the enzyme solution and another was carried out with 10 m*M* EDTA. The reaction was initiated by adding 0.67 m*M* of AHB. The progress of the reaction was followed by the decrease in absorbance of NADPH at 340 nm (measured in a 1 cm path-length quartz cell in a Cary 50 Bio spectrophotometer, Varian). The measurements were carried out every 1 s, 30 s, 30 min and 30 min for Mg^{2+}, Mn^{2+}, Ni^{2+} and Zn^{2+}, respectively, with a total reaction time of 250 s, 200 min, 2 d and 2 d, respectively. They were stopped when an equilibrium was observed (in the case of Mn^{2+}), but in the cases of Ni^{2+} and Zn^{2+} no equilibrium was reached after 2 d. In order to avoid NADPH decay owing to UV light for the long-term measurements, the cell was removed from the spectrophotometer between measurements.

In parallel with the activity measurements, the absorbance of a reference sample (protein, NADPH, cation and buffer in the same concentrations as in the sample) was followed so as to quantify the natural time-dependent degradation of NADPH. The difference in absorbance, ΔAbs, between the sample containing AHB and the reference was used in the calculation of the relative activities for each cation. This relative activity was calculated as

$$\text{Activity (\%)} = \frac{A_{\text{cation}}}{A_{\text{Mg}^{2+}}} \times 100 = \frac{\Delta\text{Abs}_{\text{cation}}}{\Delta\text{Abs}_{\text{Mg}^{2+}}} \times \frac{t_{\text{Mg}^{2+}}}{t_{\text{cation}}} \times 100,$$

where A is the activity and t is the time at which the measurement was performed. The ΔAbs of Mg^{2+} was chosen in the linear part of the curve.

3.3. Mass spectroscopy

Three samples were measured using this technique. Firstly, two crystals of the isomeroreductase/AHB/NADPH/Ni^{2+} complex were taken from a crystallization drop with a nylon loop and dissolved in 5 µl water. The estimated amount of protein molecules in the solution is 300 pmol. Secondly, 1 µl of a crystallization droplet from the same crystallization dish (*i.e.* similar concentration and time conditions) was diluted in 5 µl water. Thirdly, 1 µl of the corresponding crystallization reservoir was diluted in 5 µl water.

Several dilutions (1/3, 1/5) in H_2O/acetonitrile (20/80) (*v*/*v*) were performed prior to deposition on a matrix-assisted laser desorption ionization–time of flight (MALDI–TOF) sample plate. 0.5 µl of sample was then deposited with 0.5 µl of 2,5-dihydrobenzoic acid matrix (DHB, Sigma), yielding a further dilution of 1/2. The mixture was allowed to dry at room temperature and analysed in positive linear mode using a Voyager-Elite XL MALDI–TOF instrument (Perseptive Biosystem Inc., Framingham, MA, USA). The spectra shown represent the average of 256 laser shots (laser pulse width, 3 ns; laser wavelength, 337 nm). Acquisition conditions were as follows: accelerating voltage, 20 kV; grid voltage, 95%; guide-wire voltage, 0.3%; extraction delay, 300 ns; low-mass gate, 500 Da. The grid voltage and guide-wire voltage values are expressed as a percentage of the accelerating voltage.

3.4. X-ray data collection and quality

The data were collected at the ESRF on beamline BM14. The Mn complex was collected on a MAR300 imaging plate; a MAR345 imaging-plate detector was used for the Ni and Zn complexes. The crystals were flash-cooled at 100 K in a cryoprotectant solution containing 20% glycerol. Table 1 shows details of the data quality and refinement. The data were processed using *MOSFLM* (Leslie, 1990) and were scaled using *SCALA* (Evans, 1997).

3.5. Molecular replacement and refinement

The crystal structure of acetohydroxyacid isomeroreductase was solved by molecular replacement using the program *AMoRe* (Navaza, 1994). The search model used was one amino-terminal and one carboxy-terminal domain from the structure of acetohydroxyacid isomeroreductase complexed with NADPH, Mg^{2+} and herbicidal transition-state analogue IpOHA (Biou *et al.*, 1997). Four copies of each domain were searched for in the asymmetric unit, thus making up four monomers. The determination of the rotation and translation functions was carried out over the resolution range 10–3 Å.

Only the Mn complex was refined, as the electron-density maps showed the same features in all three complexes.

The structure refinement was carried out using *X-PLOR* version 3.851 (Brünger, 1992; Brünger *et al.*, 1987, 1990) and during the whole process 5% of the reflections were kept apart

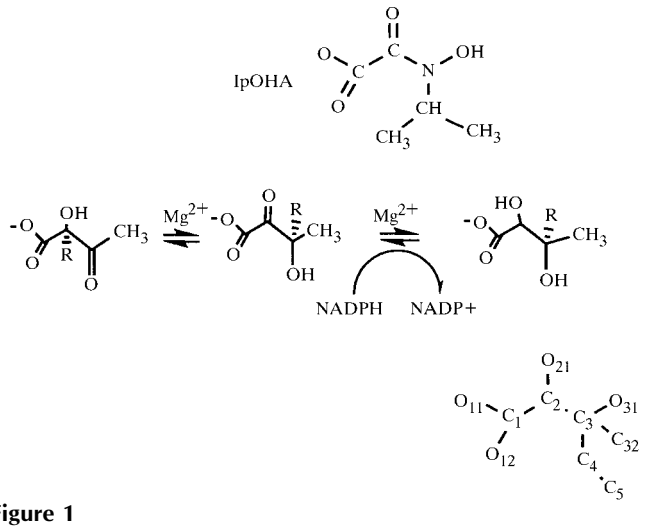

Figure 1
Reaction catalysed by acetohydroxyacid isomeroreductase. Represented above the reaction is the inhibitor IpOHA. Below: atom numbering of DHMV molecule as used in this work.

for R_{free} calculation. Structure factors for electron-density maps were calculated using *SIGMAA* (Collaborative Computational Project, Number 4, 1994) and the model building and corrections were carried out using *O* (Jones *et al.*, 1991).

The initial steps of crystallographic refinement consisted of a geometry regularization, a least-squares conjugate-gradient refinement and a rigid-body refinement at a resolution of 2.5 Å, with strict non-crystallographic constraints between the four monomers. Several cycles of refinement of atomic positions and individual temperature factors were carried out with *X-PLOR*. In parallel, the resolution was increased progressively to 1.6 Å. Each round of refinement was terminated by the calculation of a *SIGMAA* $2F_o - F_c$ map in order to view the model with computer graphics and manually correct it if necessary.

Strict non-crystallographic constraints were then replaced by harmonic non-crystallographic restraints (with k = 1256 kJ mol $^{-1}$Å^{-2}). Water molecules were then added using *PEAKMAX* (Collaborative Computational Project, Number 4, 1994). The $F_o - F_c$ map was searched for peaks greater than 3.5σ, which were attributed to water molecules if a hydrogen-bonding donor or acceptor was located within a distance of 2.5–3.5 Å. During this refinement step, simulated annealing and two applications of an overall anisotropic temperature factor were carried out. The final step of refinement consisted of progressively loosening the harmonic restraints while adding water molecules.

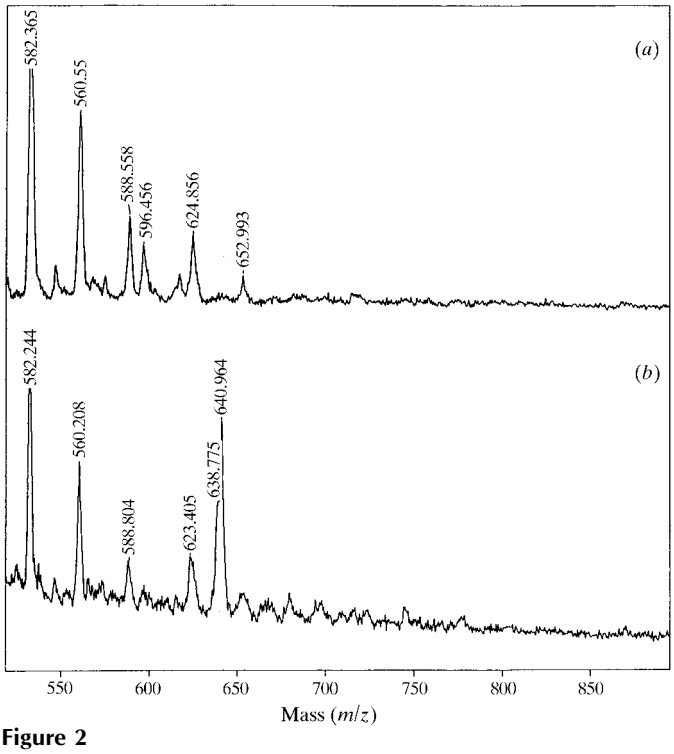

Figure 2
Mass spectra. (*a*) MALDI spectrum taken from the crystallization reservoir. (*b*) MALDI spectrum taken from a crystal of isomeroreductase/NADPH/AHB/Ni^{2+} complex. The peaks at 638 and 641 Da correspond to the NADPH degraded into (phospho)-ADP-ribose.

4. Results

4.1. Activity assays

Activity measurements were carried out in order to compare the enzyme activity in the presence of different cations. The data are shown in Table 2. The enzyme activity is ranked in the following decreasing order: Mg, Mn, no added cation, Ni, Zn. All these conditions showed the presence of some reaction. When no cation is added, a residual reaction is still observed, probably owing to trace Mg ions present as impurities in the other chemicals used. The reaction is completely inhibited by the addition of EDTA. All cations tested have a competitive inhibitory effect with respect to magnesium; Ni and Zn seem to have the strongest effect, as the reaction rate is lower with them than with no added cation.

4.2. Mass spectrometry

The purpose of the mass-spectrometry experiments was to measure the size of the nucleotide compound in the active site and to confirm its degradation into (phospho)-ADP-ribose in the crystal (see below). The method used was MALDI–TOF because of its sensitivity in the case of the dissolved crystal, as this sample contains a high salt concentration (2 *M* ammonium sulfate).

It is important to remember that the masses measured correspond to singly charged ions; therefore, 1 Da should be subtracted from the mass. Fig. 2(*a*) shows the MALDI spectrum obtained in the mass range 500–800 Da from the crystallization reservoir, which contains the precipitant solution but no protein and no NADPH. Fig. 2(*b*) shows the same spectral range measured from the dissolved crystals. The spectrum shows a major peak at a mass of 641 Da, with a shoulder at 639 Da. The calculated mass of (phospho)-ADP-ribose is 640 Da, which is identical to the major peak. The shoulder could be a doubly charged species. The mass of $NADP^+$ is 742 Da and no peak is observed in this region of the spectrum. This result shows that the 640 Da peak comes from hydrolysis of $NADP^+$. In addition, a spectrum was measured from the crystallization droplet and also shows a (phospho)-ADP-ribose peak and no peak corresponding to $NADP^+$ (data not shown).

4.3. Structure description

The structure of the complex between Mn^{2+}, (phospho)-ADP-ribose, DHMV and isomeroreductase was refined and is described here. The raw maps of the other data sets (with Ni^{2+} and Zn^{2+}) showed no striking differences and the corresponding structures were therefore not refined.

The molecular-replacement solution had an R factor of 37.7% (at 3 Å resolution), a correlation factor of 53.3% and a correct packing. The first refinement run (at 2.5 Å resolution) gave an R factor of 30.3% and an R_{free} of 31.7%. The final R factor and R_{free} are 19.3 and 22.5%, respectively.

The final model composition and geometry are described in Table 3. It is composed of four monomers in the asymmetric unit and contains 18 027 non-H atoms. The four monomers are

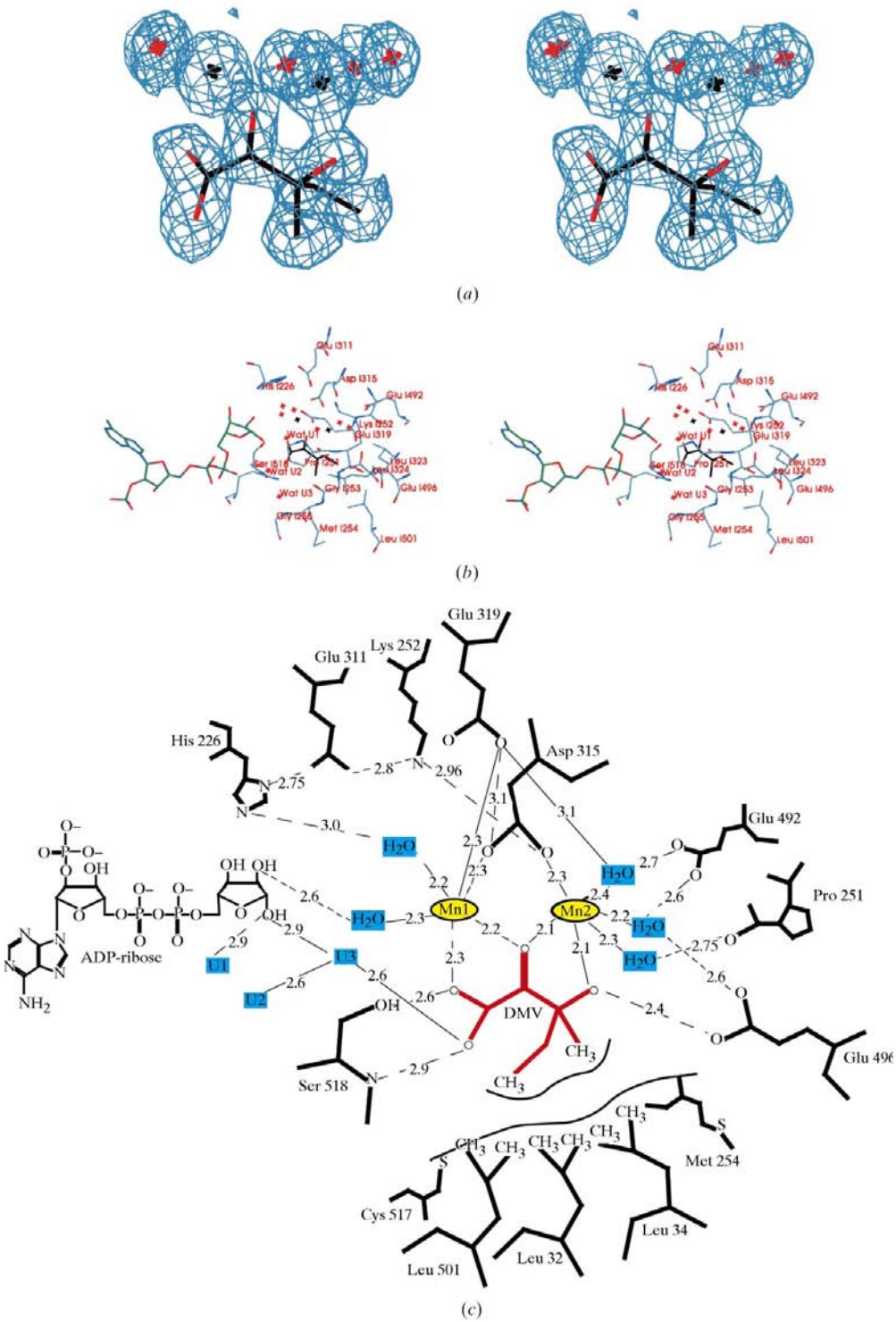

Figure 3
Active site of the isomeroreductase/Mn^{2+}/DHMV/(phospho)-ADP-ribose complex. (*a*) Stereoview showing the $2F_o - F_c$ map traced at one root-mean-square deviation around the dihydroxymethylvalerate product position. C atoms are represented in black and O atoms in red. Black crosses show the Mn^{2+} positions and red crosses represent the water molecules. (*b*) Stereoview of the residues surrounding DHMV within a 5 Å radius. The colour coding is as follows: C atoms from protein residues are in grey–blue, those from DHMV are in black and those from (phospho)-ADP-ribose are in green. All O atoms are in red and N atoms are in blue. Water molecules are represented as red crosses and Mn^{2+} ions as black crosses. Waters U1, U2 and U3 are those present in the residual density close to the former nicotinamide position. (*c*) Schematic representation of the active site, showing the distances between the ligands. The water molecules are represented in blue boxes and U1 to U3 are specified as in Fig. 3(*b*). The stereo plots were produced using the program *O* (Jones *et al.*, 1991).

designated *I* to *L*. The residue numbering includes the signal peptide. Therefore, the amino-terminal residue of the mature protein is number 72. Because of disorder of the N-terminus region in each monomer, the model presents as first residues Ser82 for monomer *I*, Phe86 for monomer *J*, Thr84 for monomer *K* and Ala83 for monomer *L*. The C-terminus is ordered and ends with the final residue Ala595 in each monomer. The Ramachandran plot (Ramachandran & Sasisekharan, 1968) assigns 93.1% of the residues to most favoured regions and no residues to disallowed regions. Three residues are in the generously allowed areas. Lys163 (monomer *J*) is located in a disordered loop and shows only patches of electron density. Conversely, Trp133 in monomers *J* and *L* are very well defined in the electron-density map. This residue is in a short loop, which may restrain its conformation. The equivalent residues in the other two monomers are in a very similar conformation and are within an acceptable region of the Ramachandran plot.

4.3.1. Overall structure. The overall structure is very similar to that of the complex with IpOHA and NADPH (Biou *et al.*, 1997; Table 4). The active site, comprising two divalent cations and the dihydroxymethyl valerate (DHMV) reaction product, is nested between the α/β amino-terminal domain and the all-α carboxy-terminal domain. The $NADP^+$ binds the N-terminal domain. However, as will be described later, the nicotinamide moiety has no density.

4.3.2. Active site. The amino-acid residues have quite similar positions to those in the IpOHA complex. However, the differences in atom positions reside in the active site, where the

Table 2
Activity assays for different cations.

The assays were performed as described in §3. The reaction rate given corresponds to a linear fit of the absorbance measurement at the beginning of the reaction. 'None', no added cation; 'EDTA', no added cation plus 10 m*M* EDTA.

Cation	Initial reaction rate (ΔDO min^{-1})†	Theoretical time required to oxidize all of NADPH‡	Activity§ (%)
Mg^{2+}	1.98	54 s	100
Mn^{2+}	3.5×10^{-2}	52 min	2.4
None	8.7×10^{-4}	34 h	0.057
Ni^{2+}	4.5×10^{-4}	67 h	0.023
Zn^{2+}	4.2×10^{-4}	72 h	0.019
EDTA	0.0	∞	0.0

† ΔOD = difference in optical density. ‡ The time given is a theoretical time corresponding to the oxidation of 1.75 nmol of NADPH by isomeroreductase at the rate given in the first column, without taking into account the competitive inhibition by $NADP^+$, supposing that the reaction is completely in the direction of the product and considering an ε value of 6250. § The activity percentage is calculated with respect to the activity in the presence of magnesium.

Table 3
Refinement results and model contents.

The r.m.s. ΔB was calculated with the program *MOLEMAN*2 for all atoms.

R factor (%)	19.3
Free *R* factor (%) (5% of reflections)	22.5
Total no. of atoms	18046
No. of protein atoms	15744
No. of solvent atoms	2090 (2089 H_2O + 1 SO_4^{2-})
No. of ligand atoms	208
R.m.s. deviations	
Bond lengths (Å)	0.008
Bond angles (°)	1.70
Dihedral angles (°)	20.55
Improper angles (°)	2.94
Average *B* factor (Å^2)	
For all atoms	15.51
For the active site	8.97
For the ligands	15.47
R.m.s. ΔB for bonded atoms (Å^2)	1.21

compound bound is DHMV and the nicotinamide moiety is absent. Fig. 3(*a*) shows the electron density around the active site. Firstly, it is obvious that the ethyl chain (C4—C5) is bound to the distal C3 and not to the middle C2 as in the substrate. Therefore, alkyl transfer has taken place. Secondly, the high resolution of this electron-density map shows that the conformation of the middle carbon is tetrahedral and not planar as it would be in the intermediate compound. Therefore, complete reaction has taken place and we observe the complex with the DHMV product, Mn^{2+} ions and (phospho)-ADP-ribose. Fig. 3(*b*) shows a stereoview of the active site and Fig. 3(*c*) shows a detailed schematic with the interatomic distances. The DHMV molecule makes extensive interactions with its neighbours: it makes electrostatic interactions with both Mn^{2+} cations and with Ser518 and Glu496, and is in close proximity to water molecules. In addition, the apolar moiety of DHMV is surrounded by a hydrophobic cluster of C and S atoms (Cys517, Leu501, Leu323, Leu324 and Met254). The manganese cations exhibit a hexagonal bipyramidal conformation and are bridged by Asp315. They are in contact with water molecules, which in turn are hydrogen bonded to polar side chains.

4.3.3. $NADP^+$ density. The electron density for the whole of $NADP^+$ is clear except for the nicotinamide ring, where it is very low (Fig. 4). Occupancy coefficients for the ring atoms were refined while fixing their temperature factors at a value of 13 Å^2, which corresponds to the average of the surrounding atoms. This led to occupancy coefficients of the order of 0.25. The *R* factor at this stage was 20.0% ($R_{\rm free}$ = 23.0%). The omit map calculated in the absence of NADPH shows two densities close to the nicotinamide ring: a spherical density close to C5N and a croissant-shaped density close to the amide position (Fig. 4). The first density was refined as one water molecule (named U1 in Figs. 3*b* and 3*c*) with an occupancy of 0.54 and the second one as two waters (U2 and U3) with occupancies of 0.51 and 0.68. The *R* factor then fell to 19.5% ($R_{\rm free}$ = 22.7%). The third possibility we tried was to insert an amide (NH—CH_2—O) group, which refined with an occupancy of 0.4. However, the presence of an amide group alone is unlikely, as the degradation of the NADPH into (phospho)-ADP-ribose removes the whole nicotinamide group, as seen from the mass-spectrometry results. In addition, this raised both the *R* factor and $R_{\rm free}$ significantly. As a consequence, the $NADP^+$ was replaced by a (phospho)-ADP-ribose in the final model.

4.4. Comparison with the Ir/Mg^{2+}/IpOHA/NADPH complex

The structure outside the active site is very similar in both complexes; most variations are at the surface of the protein where residues are more flexible and therefore are not very significant. At the active site, most side chains have equivalent positions with variations in the interatomic distances. The equivalent regions of IpOHA and DHMV, namely the carboxylate and the apolar moieties, are in the same positions. The hydroxamate in IpOHA is positioned at the site of the C3 of DHMV (see Fig. 1). Around the nicotinamide position, the side chain of Asn136 has moved towards the former nicotinamide position and the additional water molecules. Its NE2 atom is within hydrogen-bonding distance of one of those water molecules and of the carboxylate O atom of Gly253.

5. Discussion

We determined the structure of acetohydroxyacid isomeroreductase complexed with its reaction product, (phospho)-ADP-ribose and several divalent cations. The electron-density map shows in great detail the interaction between the enzyme and its product. The intriguing facts about this structure are on one hand the completeness of the reaction in spite of very unfavourable conditions (presence of divalent cations which slowed the reaction down by a factor of 2000) and on the other hand the observation of the degradation of the $NADP^+$ to (phospho)-ADP-ribose.

Table 4
Comparison between the Mg/NADPH/IpOHA (Biou *et al.*, 1997) and Mn/(phospho)-ADP-ribose/DHMV (this work) complexes.

The r.m.s.d.s between the model with Mg^{2+} and the model with Mn^{2+} are calculated for all atoms of the tetramer and of the four monomers (*I*, *J*, *K* and *L*). The numbers in brackets are the r.m.s.d.s between C^{α} atoms.

	Tetramer	Monomer *I*	Monomer *J*	Monomer *K*	Monomer *L*
R.m.s.d.	0.71 (0.43)	0.48 (0.24)	0.55 (0.23)	0.57 (0.24)	0.63 (0.34)

5.1. Presence of the reaction product in all of the crystals: is the enzyme more stable when complexed to its product?

We observe 100% of reaction product bound to the enzyme in all three conditions, even with Zn^{2+}, where the reaction is extremely slow. On the other hand, although we have obtained crystals with IpOHA and Mg^{2+} without NADPH, no diffraction-quality crystals were obtained with substrate AHB, Mg^{2+} and no NADPH or with no ligand at all (unpublished results). In addition, a minimum of two divalent cations per enzyme monomer is necessary and sufficient to obtain crystals with IpOHA and NADPH (Dumas *et al.*, 1994).

Furthermore, hydrogen/deuterium combined with mass-spectrometry experiments have shown there to be a large conformational change between the free enzyme and its complexed states (Halgand *et al.*, 1999). Therefore, it seems that the free enzyme is not in a sufficiently stable state to yield crystals. The free state is more agitated, with both domains lacking cohesion with respect to each other. This cohesion is brought mainly by the binding of the NADPH, which links both domains, and of the cations, which are an intrinsic part of the substrate-binding site. When the substrate binds to the enzyme, the reaction is ready to occur and is observed to have occurred in all of the crystals we have measured. In principle, we should end up with an equilibrium where the excess $NADP^+$ inhibits the enzyme, so we should have a mixture of substrate and product. However, the $NADP^+$ is degraded in the crystals and in the crystallization drop and no complete NADPH or $NADP^+$ is observed. Moreover, this high-resolution structure was refined with 100% occupancy of the reaction product DHMV. Thus, it seems that all of the AHB has been converted into DHMV and all of the NADPH has been converted into (phospho)-ADP-ribose in the crystals. This was confirmed by complementary experiments.

5.2. Low electron density at the nicotinamide position

An absence of density for the nicotinamide moiety of $NADP^+$ when involved in a reaction-product complex has been observed previously (Karplus & Schulz, 1989; Stoddard & Koshland, 1993). It was also observed for a mutant of glyceraldehyde 3-phosphate dehydrogenase for which the NAD^+ nicotinamide has no density (Ollivier, 1994). In addition, Pai *et al.* (1988) observed a decrease in nicotinamide occupancy in glutathione reductase complexes. The absence of electron density could be a consequence either of disorder or of degradation of the nicotinamide cofactor. The disorder hypothesis is unlikely in our case, as the only possibility would be a rotation around the C1′A—N9A bond, but there is no space for the nicotinamide ring to rotate freely in the NADPH-binding site of isomeroreductase. On the other hand, the hydrolysis of the NADPH to (phospho)-ADP-ribose [$NAD(P)^+ + H_2O \rightarrow$ (phospho)-ADP-ribose + nicotinamide] is possible. Such a reaction occurs *in vivo* through an enzyme $NADP^+$ nucleosidase (E.C. 3.2.2.6). Mass-spectrometry measurements were performed on dissolved crystals to verify the degradation of $NADP^+$ that was observed in the electron-density map. These measurements confirmed the hydrolysis of $NADP^+$ to (phospho)-ADP-ribose. To our knowledge, this is the first time that such a hydrolysis occurring in crystals of reaction-product complex has been interpreted and confirmed by complementary experiments.

As a conclusion, X-ray crystallography and mass spectrometry show that the $NADP^+$ is unstable and is degraded into (phospho)-ADP-ribose.

5.3. Proposal for a reaction mechanism

The present structure shows the end of the reaction transforming 2-aceto-2-hydroxybutyrate into 2,3-dihydroxy-3-methylvalerate. In an earlier paper, we published a hypothesis for the reaction (Dumas *et al.*, 1995). Combining the information obtained from the present structure with that of the complex with the intermediate-state analogue IpOHA (Biou *et al.*, 1997), we propose a reaction scheme. In the first step (Fig. 5*a*), the isomerization reaction could be started by the action of Glu496 and Mg2, which polarize the carbonyl group on the C3 of AHB (see atom numbering in Fig. 1). A hydroxyl group may participate in the rearrangement process by removing a proton from the substrate O21 hydroxyl group. This hydroxyl group could come from a deprotonated water molecule. This deprotonation would be made easier by the two magnesium ions coordinated to the O atom. The proton removed from O21 goes to O31. The transition state of the isomerization, shown in Fig. 5(*b*), is thought to present a transient bridged alkyl function. The accommodation of two different alkyl chains is made easier by the apolar environment around the C atoms C4–C5 and C32 area (see Figs. 3*b* and 3*c*). The beginning of the NADPH-catalysed reduction (Fig. 5*c*) is equivalent to the IpOHA complex. During this step, the hydride transfer is made easier by the polarizing effect of the magnesium ions upon the reaction intermediate carbonyl function. The last step (Fig. 5*d*) shows the present structure with the full $NADP^+$ instead of (phospho)-ADP-ribose and with DHMV in the active site. Further experiments are needed to understand better this complex two-step reaction. In particular, the functions of the two basic residues His226 and Lys252, which are close to the active site, need to be clarified.

5.4. Difference between enzymology and crystallization time scales

In this work, we obtained a reaction-product complex where the input compound was the substrate and the reaction

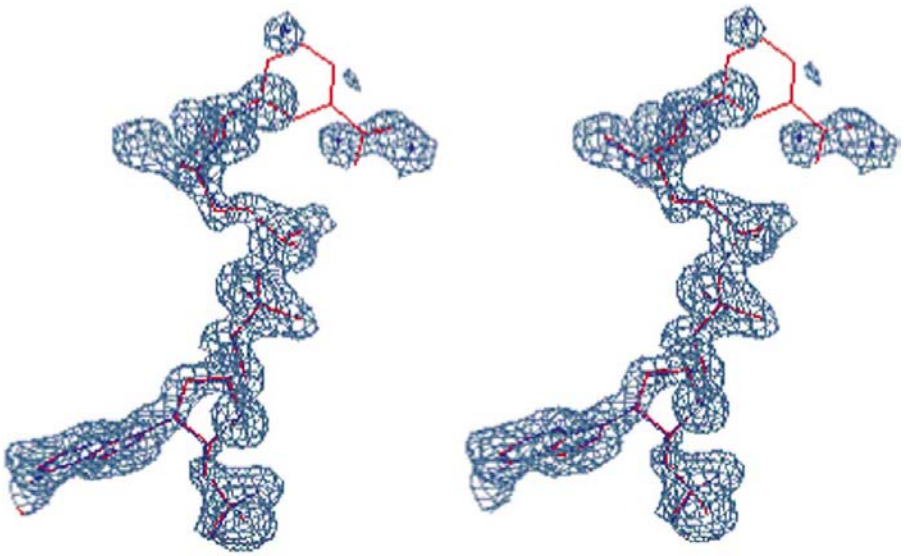

Figure 4
Stereoview showing the OMIT map calculated without the NADPH and atoms surrounding it within 3.5 Å. The map is contoured at the 1σ level. The NADPH as refined at the beginning of the refinement is shown in red and the (phospho)-ADP-ribose and the three water molecules are shown in black. The image was produced using the program *O* (Jones *et al.*, 1991).

conditions were unfavourable. On the time scale required to obtain macromolecular crystals (in the present case, 3–4 d), the initial reaction rate is sufficient for the reaction to take place in all of the complexes. Considering that the measurements were all performed on crystals which were more than one month old, the reaction has had even more time to take place.

This study confirms that crystallized proteins are often very active, even at a pH different from their optimal functional pH (8.2 for the isomeroreductase) and at high salt concentrations. The most striking example is the Zn^{2+} case, where the reaction is extremely slow but is still complete in the crystals. We cannot rule out that the reaction was partly a consequence of trace magnesium ions, as no reaction at all was observed in the

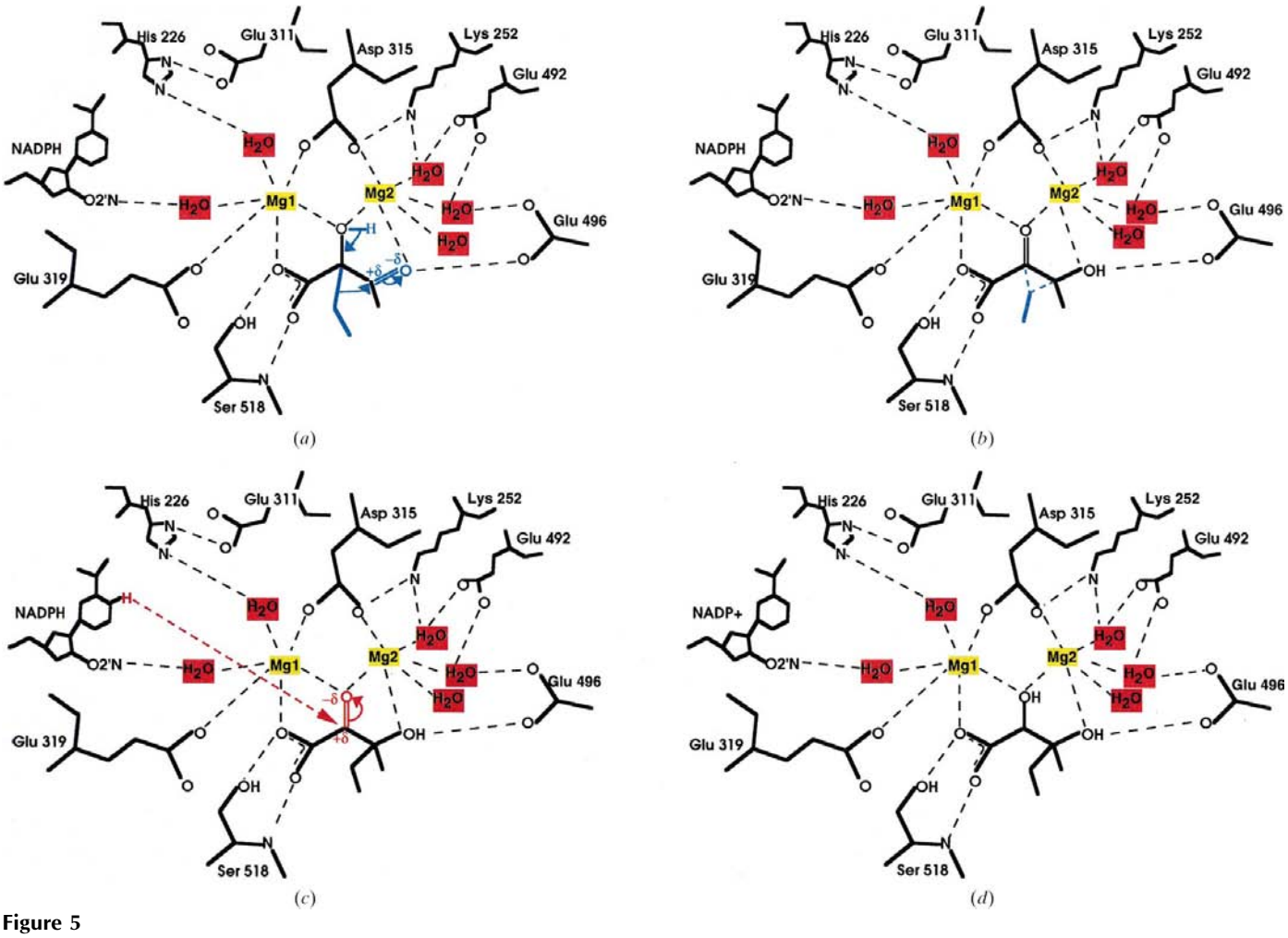

Figure 5
Proposal for a reaction scheme. The blue regions show atoms involved in the first reaction step (isomerization) and the red regions show those involved in the reduction step. Black dashed lines show the electrostatic interactions and blue dashed lines in (*b*) indicate an intermediate state, where the ethyl group is bridged between two C atoms. See text for comments.

presence of EDTA, while we still observed a partial reaction when no cation was added.

We thank Andy Thompson for his help in data collection on beamline BM14 at the ESRF, Eva Pebay-Peyroula and Claudine Cohen-Addad for useful comments, and Emile Duée for discussions on the stability of NADPH. This work was supported in part by a thesis grant to KT from Ministère de l'Education Nationale, de la Recherche et de la Technologie and by a thesis grant to FH from Rhône-Poulenc. It was initiated under the Bioavenir program financed by Rhône-Poulenc with contributions from CNRS.

References

Biou, V., Dumas, R., Cohen-Addad, C., Douce, R., Job, D. & Pebay-Peyroula, E. (1997). *EMBO J.* **16**, 3405–3415.
Brünger, A. T. (1992). *Nature (London)*, **355**, 472–474.
Brünger, A. T., Krukowski, A. & Erickson, J. (1990). *Acta Cryst.* A**46**, 585–593.
Brünger, A. T., Kuriyan, J. & Karplus, M. (1987). *Science*, **235**, 458–460.
Collaborative Computational Project, Number 4 (1994). *Acta Cryst.* D**50**, 760–763.
Dumas, R., Butikofer, M.-C., Job, D. & Douce, R. (1995). *Biochemistry*, **34**, 6026–6036.
Dumas, R., Job, D., Douce, R., Pebay-Peyroula, E. & Cohen-Addad, C. (1994). *J. Mol. Biol.* **242**, 578–581.
Dumas, R., Job, D., Ortholand, J.-Y., Emeric, G., Greiner, A. & Douce, R. (1992). *Biochem. J.* **288**, 865–874.
Evans, P. R. (1997). *Proceedings of the CCP4 Study Weekend. Recent Advances in Phasing*, edited by K. S. Wilson, G. Davies, A. W. Ashton & S. Bailey, pp. 97–102. Warrington: Daresbury Laboratory.
Halgand, F., Dumas, R., Biou, V., Andrieu, J. P., Thomazeau, K., Gagnon, J., Douce, R. & Forest, E. (1999). *Biochemistry*, **38**(19), 6025–6034.
Jones, T. A., Zou, J. Y., Cowan, S. W. & Kjeldgaard, M. (1991). *Acta Cryst.* A**47**, 110–119.
Karplus, P. A. & Schulz, G. E. (1989). *J. Mol. Biol.* **210**(1), 163–180.
Leslie, A. G. W. (1990). *Crystallographic Computing 5. From Chemistry to Biology*, edited by D. Moras, A. D. Podjarny & J.-C. Thierry, pp. 50–61. New York: Oxford Science Publications.
Navaza, J. (1994). *Acta Cryst.* A**50**, 157–163.
Ollivier, L. (1994). PhD thesis, Doctorat de l'Université Joseph Fourier Grenoble, France.
Pai, E. F., Karplus, P. A. & Schulz, G. E. (1988). *Biochemistry*, **27**, 4465–4474.
Ramachandran, G. N. & Sasisekharan, V. (1968). *Adv. Protein Chem.* **23**, 283–437.
Stoddard, B. L. & Koshland, D. E. Jr (1993). *Biochemistry*, **32**, 9317–9322.
Sylvester, S. R. & Stevens, C. M. (1979). *Biochemistry*, **18**, 4529–4531.